

OPEN ACCESS

Mechanical nano-structuration of a C45 steel under repeated normal impacts

To cite this article: G Kermouche and C Langlade 2014 *IOP Conf. Ser.: Mater. Sci. Eng.* **63** 012019

View the [article online](#) for updates and enhancements.

You may also like

- [Migration of tungsten dust in tokamaks: role of dust-wall collisions](#)
S. Ratynskaia, L. Vignitchouk, P. Tolias et al.
- [Molecular modeling of Ti-6Al-4V alloy shot peening: the effects of diameter and velocity of shot particles and force field on mechanical properties and residual stress](#)
Ali Moradi, Ali Heidari, Kamran Amini et al.
- [Experimental study on mechanical property and stone-chip resistance of automotive coatings](#)
Yang Liu, Chenqi Zou, Mengyan Zang et al.





The
Electrochemical
Society

Advancing solid state &
electrochemical science & technology

DISCOVER
how sustainability
intersects with
electrochemistry & solid
state science research

Mechanical nano-structuration of a C45 steel under repeated normal impacts

G Kermouche¹ and C Langlade²

¹ Ecole des Mines de Saint-Etienne, SMS division, LGF UMR CNRS 5307, 158 Cours Fauriel 42023 Saint-Etienne, France

² Université Technologique de Belfort-Montbéliard, IRTES-LERMPS EA 3316, 90 010 Belfort Cedex, France

E-mail: kermouche@emse.fr; cecile.langlade@utbm.fr

Abstract. Under repeated impact loadings that are encountered during peening process, surface mechanical attrition treatment or erosive wear, metals undergo severe plastic deformation which may lead to a local refinement of their microstructure in the near-surface. These mechanically-induced surface nano-structures exhibit very interesting physical properties such as high hardness and better tribological properties, ... Strong research efforts have been undertaken during the last years to understand the mechanism explaining how these nanostructures are created and grow under such loadings. It is commonly accepted that the shear stress induced by oblique impacts is the driving force for such mechanical transformations. Nevertheless, we have recently observed that normal impacts may also lead to such grain refinement. In this paper, this mechanism is investigated on a AISI1045 steel submitted to different heat treatments. A phenomenological mechanism based on a previous work is presented and shows a good efficiency on the air cooled sample. Nevertheless it failed to explain the differences observed between the different samples, showing the necessity to take into account both the material stress-strain curve and the microstructural state.

1. Introduction

Under severe cyclic solicitations, most metallic or ceramic materials undergo high plastic deformation that leads to microstructural modifications and to wear [1–13]. These structural transformations of the subsurface layers, called TTS (Tribologically Transformed Structure) or MAS (Mechanically Attrited Structure) or also MML (Mechanically Mixed Layer), have been widely studied in the past, especially in the case of bearing or rail applications. However, they may be encountered in most tribological contacts, even under very mild conditions. In some studies, researchers were mainly interested in understanding the wear mechanisms and controlling the wear rate [2,5]. However, the formation phenomenon has also been investigated without clear identification of a specific mechanism. In particular, two main hypotheses have been proposed. The first one is mainly based on the mechanical approach neglecting the role of the counterface and environment and mainly considering the plastic behaviour (including plastic deformation and substructures, shear bands...) [6–8]. The second one considers the role of the material and environment chemistry and explores scenario involving mechanical alloying and material mixing [12,13]. The various names used to present the material transformation reflect the still open question. However TTS structures have recently raised new interest not only due to their very high hardness but also because of their nanocrystalline structure leading to specific properties and new surface treatments referred to as SMAT (Surface Mechanical Attrition Treatment) and *NanoPeening*[®] have been patented [6–10]. For these last studies, the effects of the SMAT treatment are investigated in terms of microstructural, residual stress and corrosion resistance changes but no clear scenario is proposed to explain the material evolution as a function of the SMAT conditions. One of the main problems of all these studies is the very limited amount of transformed matter that prevents from any extensive and reproducible TTS analyses. In the case of the SMAT treated surfaces, the study of the produced



nanocrystalline material is largely restrained by the limited knowledge of the experimental parameters.

It is commonly accepted that the shear stress induced by oblique impacts is the driving force for such mechanical transformations [7,8]. Nevertheless, we have recently observed [1, 11] that normal impacts may also lead to such grain refinement (Fig 1) on different steels and alloys. With such kind of loading, significant amount of TTS can be created contrary to most of impact based processes. Nevertheless the way the TTS is formed remains unclear. In this paper, this mechanism is investigated on a AISI1045 steel submitted to different heat treatments in order to highlight the effect of the initial microstructure and hardness on the TTS growth kinetics.

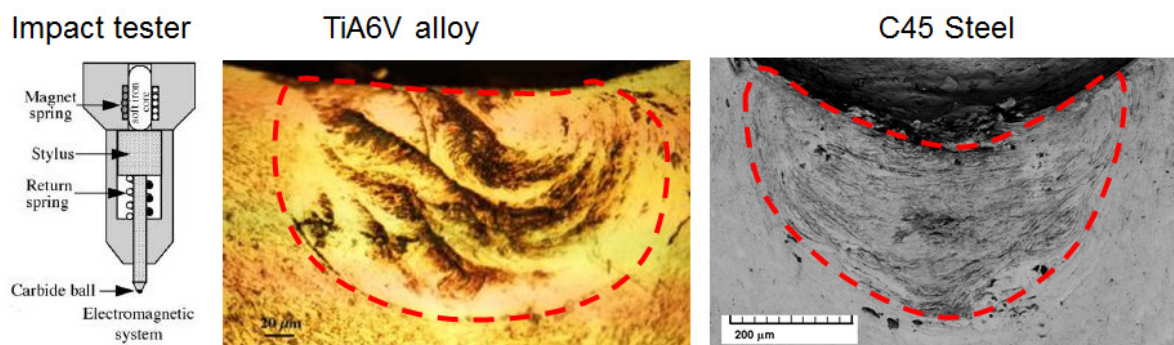


Fig. 1 – micro-impact set up, 2 – Cross-sections of repeated impact-induced Tribologically Transformed Structures in a TiA6V alloy and in a C45 (AISI1045) steel after 5000 impacts [1;11]

2. Materials and methods

2.1. Impact tests

Micro impact tests with energy control have been performed using the device developed in [14,15] and sketch on Fig 1. Indenters made of cermets (WC + Co, provided by Technifor) terminated by a hemi-spherical part of 100 µm or 500 µm radius were used. Depending on the electromagnet control and the initial position of the tip above the sample surface, the incident tip velocity and associated kinetic energy may be adjusted to obtain the desired induced normal load. In the present study, the estimated impacting energies were ranging from 0.5 to 9 mJ leading to induced normal loads F_n of 200 to 2000 N. The impacting frequency was fixed to 10 Hz and the number of impacts (N) can be adjusted from isolated (single) impact to several 10^6 cycles. Previous simulations have clearly shown that no heating effect are generated during such impact tests and a maximum temperature increase of less than 60°C has been estimated [11].

2.2. Materials

The reference material studied is a standard (AISI1045) C45 steel (0.46% w C, 0.7%w Mn, 0.2% w Si, 0.17% w Cr, 0.05% w Ni). To study the influence of its initial microstructure on its ability to form a TTS sublayer, several heat treatments have been performed. All samples have been thermally treated at 850°C for 20 minutes to obtain an austenite phase. After this austenitization step, four different cooling and tempering treatments have been performed. After heat treatment, all samples were machined in order to suppress the possible decarburized layer and polished to obtain a mirror finish (SiC paper up to grade 1200 + 3 and 1 µm diamond grids). Fig 2 presents the typical microstructures obtained after the four different thermal treatments (Nital 3% etching). The air-cooled sample noted C45A shows a classical ferrite-pearlitic structure with a mean grain size of around 10 µm. After water quenching (C45W), the C45 steel is fully martensitic and tempered martensite is observed for

the samples after 1h tempering at 450°C (C45WT4), and 575°C (C45WT5). Just prior to any impact testing, the mirror polished surfaces were finally cleaned with ethanol in an Ultra-Sonic bath.

2.3. Characterization

For the TTS observation, samples were cross-sectioned, mirror polished and etched (Nital 3%) after each series of impacts.

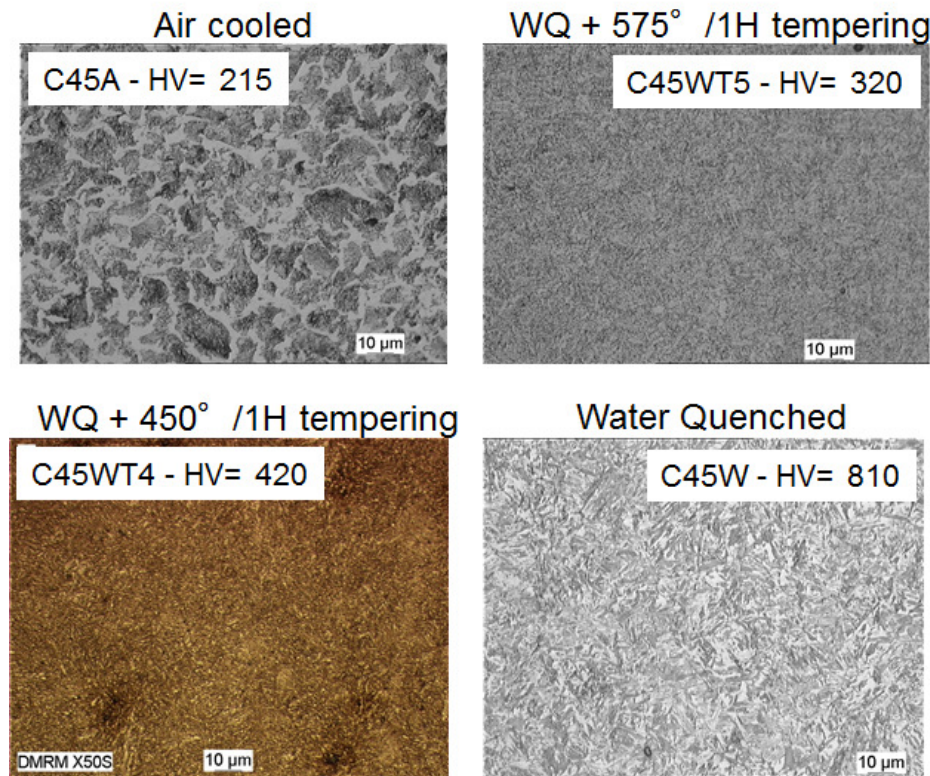


Fig 2 - Optical micrographs of the AISI1045 microstructures for the different heat treatments

3. TTS growth mechanism and air cooled sample

A mechanism was recently proposed to explain the growth mechanism of TTS in a AISI1045 Steel by repeated normal impacts, based on a FE analysis of the multiple impacts [11]. It was observed that there was a strong correlation between the zone where Severe Plastic Deformations occur and the TTS. In this zone, the cumulated plastic strain increases at each impact and can reach large values even in the stabilized impact regime – i.e. when the impact scare is no more affected by the repeated impacts - due to the presence of reversal plastic strain [16-17]. This cumulative plastic deformation during the stabilized impact regime was interpreted as a local mechanical mixing of the material. As suggested by Lu et al [6-9], the plastic strain induced grain refinement process under impact conditions is due to the combination of the large plastic strain reached locally and the high strain rates induced by the impacts (between 100 s⁻¹ and 1000 s⁻¹). Hence, when plastic deformation reaches a given value, nanocrystalline structures may be created. The TTS is very hard, thus, it acts as a new indenter on the region below, which will also be transformed into a TTS following the same mechanism. Consequently TTS should grow progressively, starting from the surface as sketched on Fig 3.

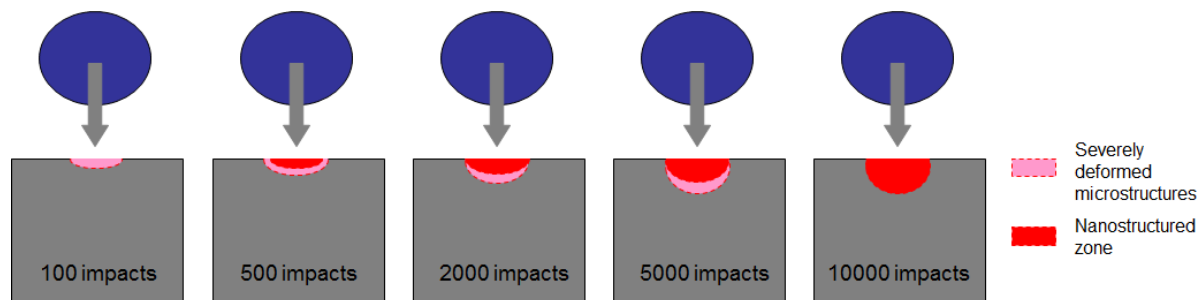


Fig 3 – Mechanism proposed by Kermouche et al [11] to explain the creation and the growth of TTS under repeated impact tests

The main parameters governing the formation of TTS zones using this mechanism appears to be the number of cycles and also the kinetic energy of the indenter in relation with the strain hardening of the material. It was also shown that the rise of temperature during one impact is not high enough to induce alone structural changes in the material and that the main effect of the high hydrostatic pressure is to ensure that the material could undergo this severe plastic deformation in preventing damaging phenomena. It shall be noted that this model suffers of a strong limitation because it is only based on the macroscopic stress-strain curve and not on microstructural related quantities such as dislocation densities (SSD, GND) or grain size distribution [17-21]. Nevertheless, as shown in Fig4 , it leads to very satisfying agreements for the air cooled C45 in assuming that the plastic strain threshold for the nanocrystallisation onset is close to 2.0. This strain level may appear as not large enough to result in mechanical nanostructuration with common SPD treatments. This shall be a consequence of the complex strain path, the high strain rate and plastic strain loops induced by the repeated impacts which can promote the dislocation cell population increase. More details on the Finite Element Analysis can be found in our previous paper [11].

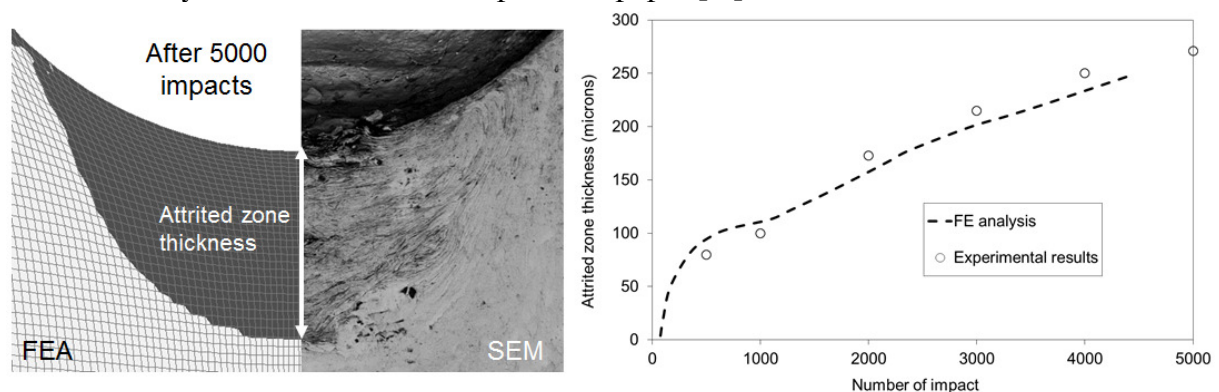


Fig 4 : Left – TTS shape predicted with FEA and compared to the one observed on the C45 steel annealed (BS –SEM image). Right - Evolution of the TTS thickness as a function of the number of impacts. The plastic strain threshold for the creation of TTS is set to 2.0 in the FEA.

One question dealing with this mechanism is the apparent necessity to repeat impacts to create the TTS. It could be formulated as follows: “Is it possible to create such Mechanically Attrited Structure using a single high energy indentation test?” To address this issue in a simple way, we investigate the microstructure evolution induced by the deep indentation of a hardened AISI52100 1 mm diameter ball in the air cooled C45. This test was performed using a 100 kN compression set-up.

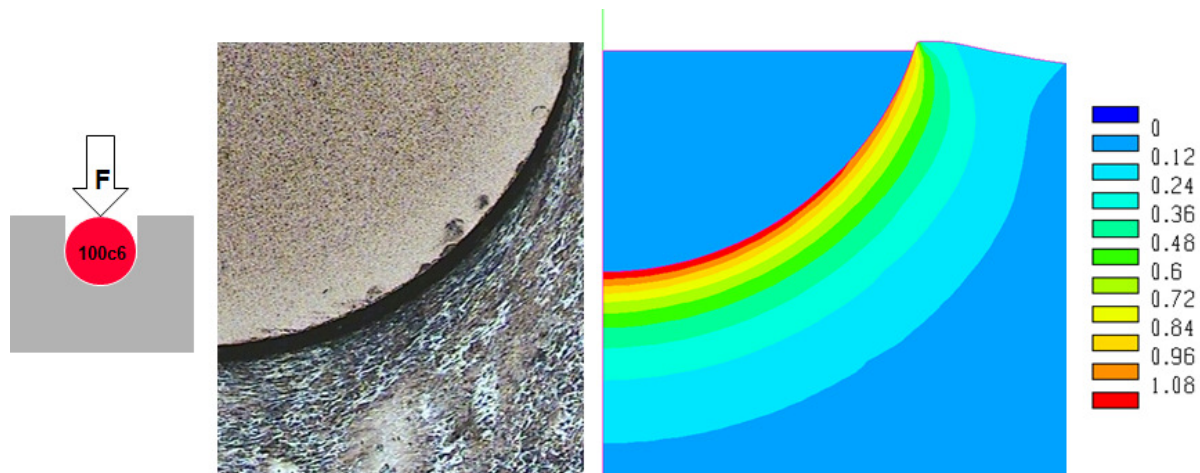


Fig 5 - deep indentation of an hardened AISI52100 (100c6) in the air cooled C45 steel. No significant TTS have been observed. FEA reveals that the plastic strain level induced by this loading is not high enough to result in TTS formation, contrary to repeated indentation.

As shown on Fig 5, there is almost no TTS created by such a process or just a small amount that cannot be identified through an optical micrography. This is correlated to the plastic strain level resulting of the deep indentation finite element analysis. The impact score is the largest as possible because the ball was fully embedded in the C45 steel after the test. By referring to classic indentation theory where the equivalent strain is computed as the ratio of the indent score and the ball radius [22], it means that the plastic strain level should be higher in the case of deep indentation. It underlines the importance to take into account the reversal plastic strain induced by the loading/unloading cycles. One may ask about the effect of the strain rate which is known to influence nanocrystallisation by severe plastic deformation [9]. The equivalent strain rate, computed as the ratio between the indentation rate over the ball radius [22] was estimated to be close to 10 s^{-1} with the deep indentation test, which is lower than the equivalent impact strain rate ($100 - 1000 \text{ s}^{-1}$). However it is not so drastically different and thus cannot explain alone the difference observed in terms of microstructure.

4. Heat treatment effect on the TTS creation.

The TTS revealed after 7000 impacts is shown on Fig 6. A first conclusion is that the TTS shape is strongly related to the Hardness. For the Water Quenched samples (C45W), there is almost zero TTS after 7000 impacts but a significant amount exists after 1000 impacts (Fig 7). It can be seen that the TTS area for all samples is not homogeneous and the ferrite-perlitic structure may still be observed, even if the grains appear to have a drastically reduced grain size and are highly deformed. This modified structure exhibits a typical foliated structure. It can be noted that a highly fractured and coarse layered structure may be observed at the subsurface (Fig 7). EDS analyzes (not shown in this paper) have revealed the high oxygen content of some lamellae, which suggests the presence of Fe_2O_3 iron oxides in the foliated structure. It has to be noted that this oxygen presence may be observed at depth as high that microns where no direct contamination could be imagined. It therefore suggests the occurrence of significant matter flow in the affected area confirming the severe plastic deformation induced by the repeated impact and the mechanism proposed in [11].

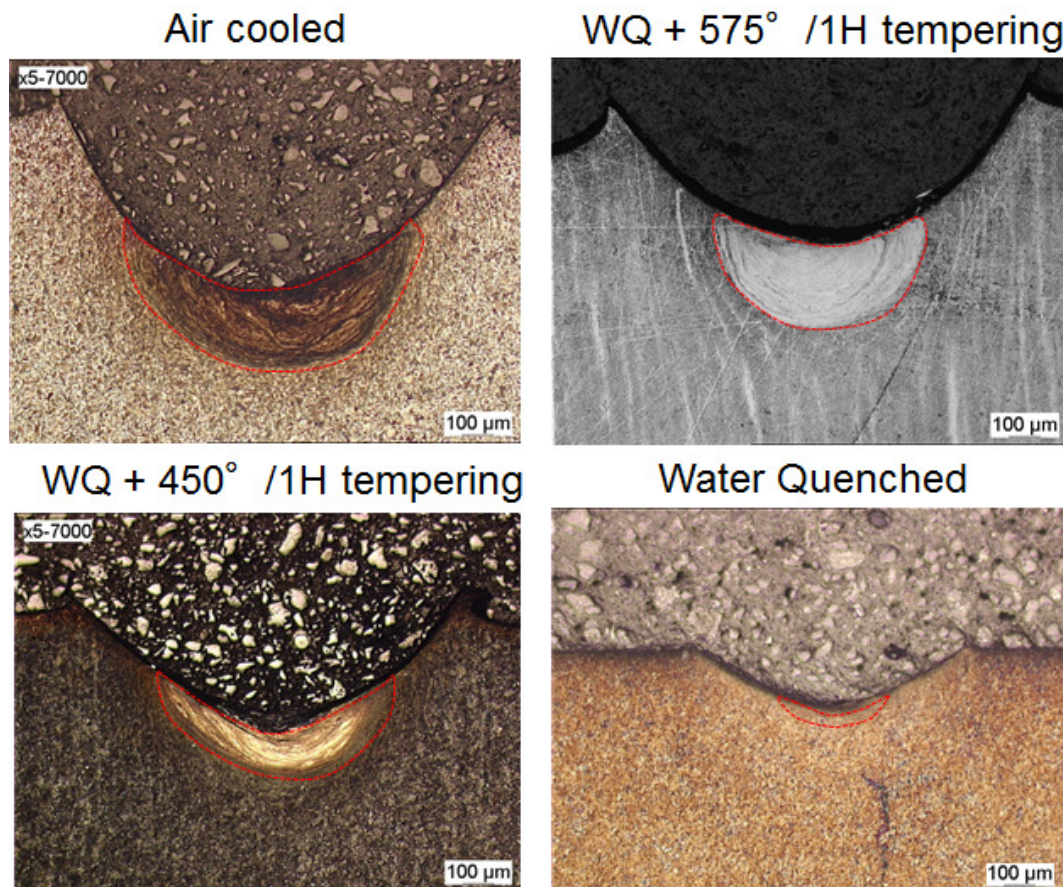


Fig. 6 : TTS shape after 7000 impacts for the different heat treatments.

The TTS thickness as a function of the number of impact is plotted on Fig 7. It can be noticed that for the Water Quenched Sample, there is a TTS formed during the first 1000 impacts then it is progressively removed by the following impacts. This could be interpreted as a consequence of the TTS brittleness inducing a bad resistance to erosive wear under normal incidence. This conclusion can also be drawn for the other heat treatments but with an erosive wear process starting at a higher number of impacts. Let us note that the TTS thickness after 30000 impacts is almost similar for samples C45A, C45WT4 and C45WT5.

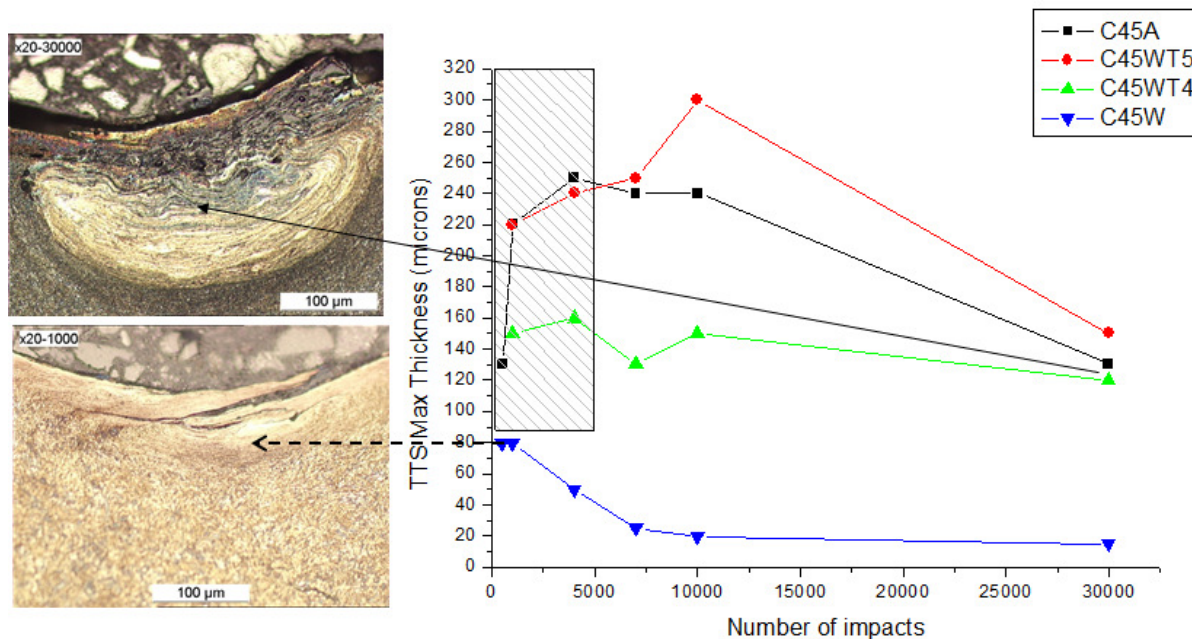


Fig. 7 : Evolution of the TTS thickness as a function of the number of impact for different heat treatments.

These results highlight that the TTS thickness and its growth with the number of impacts is governed by the hardness (and thus the ductility). By comparing the result on the samples C45A (215 Hv), C45WT4 (420 Hv) and C45W (810 Hv), it is possible to conclude that the higher the hardness, the lower the TTS thickness. Nevertheless this simplistic explanation fails if one tries to compare the results on the samples C45A (215 Hv) and C45WT5 (320 Hv), where the TTS growth is almost similar even though the hardness of the C45WT5 is 50% higher. As the Vickers hardness is related to a single point of the stress-strain curve (i.e. the stress for a plastic strain around 8% [23,24]), it is not able to give a full account of the cold hardening capability. For that purpose, we recently developed a method based on repeated micro-impact tests to measure the stress-strain curve in strain rate range in relation with the impact tests [22]. The stress-strain curve for each sample is plotted on Fig 8. Surprisingly, the samples C45WT4 and C45W exhibit the same stress-strain dependencies and not the samples C45WT5 and C45A as we could expect from the results of Fig 7. Only one conclusion can be drawn from these results: a one-to-one correspondence between the TTS growth and the stress-strain curves cannot be found. Consequently, it is necessary to take into account physical parameters such as lattice curvature and/or grain size distribution to model correctly this phenomenon such as the model developed for dynamic recrystallization [21] or SPD-induced nanocrystallisation [19,20].

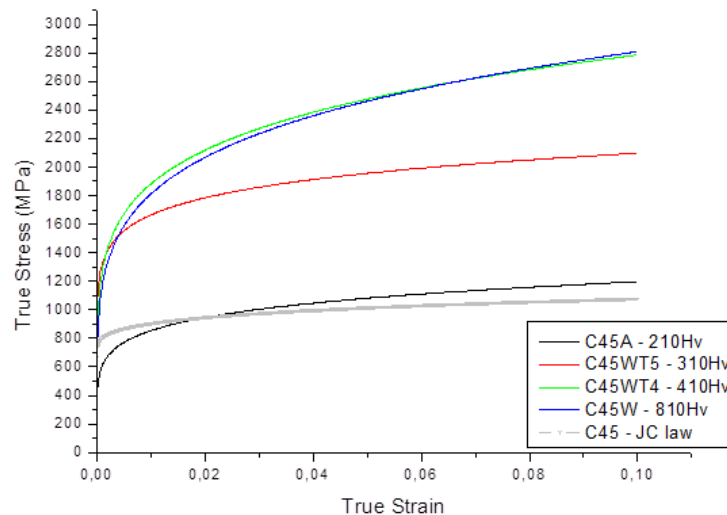


Fig. 8 : Stress-strain curves at 100 s⁻¹ measured using the repeated impact set up and the procedure described in [22]. The JC law refers to the stress-strain curve identified with a Hopkinson bar device [25].

5. Conclusion

It is shown in this paper that

- SPD-induced nanocrystallisation (or Tribologically Transformed Structure) may happen under repeated normal micro-impacts such as in the case of impact-based surface mechanical treatment (SMAT, *NanoPeening*[®], ...),
- significant amount of TTS can be created contrary to most of impact based processes,
- the first TTS amount is created after a given number of cycles when a critical value of the cumulated plastic deformation is reached (plastic shakedown). Then the newly formed TTS acts as an indenter on the region below, which will also be transformed into a TTS following the same mechanism,
- single deep indentation could not produce TTS whatever the load applied on the indenter showing that the reversal plastic strain during the loading/unloading cycles play a major role,
- there is a maximum thickness of TTS depending on the surface hardness and the impact conditions,
- for high impact numbers, erosive wear lead to a decrease of the TTS thickness, thus a critical number of impacts can be defined to optimize the TTS amount,
- there is apparently not a one-to-one relation between the TTS growth and the stress-strain curves indicating that physical parameters such as the GND dislocation density have to be taken into account to simulate the TTS growth accurately.

More generally, it is shown that the use of micro-percussion devices could make possible to reach an improved understanding of impact-based processes as the TTS growth kinetics can be directly related to impact conditions (impact energy, indenter radius, location) contrary to SMAT or *NanoPeening*[®] process

6. References

- [1] A.C. Sekkal, C. Langlade, A.B. Vannes. 2005 *Mat. Sci. & Eng. A* **393** 140
- [2] J.E. Morgan 1983 *Wear* **84** 51

- [3] E. Sauger, L. Ponsonnet, J.M. Martin, L. Vincent 2000 *Tribo. Int.* **33** 743
- [4] M. Busquet, S. Descartes, Y. Berthier 2009 *Tribo. Int.* **42**, 1730
- [5] G. Kermouche, A.L. Kaiser, P. Gilles, J.M. Bergheau 2007 *Wear* **263** 1551
- [6] K. Lu, J. Lu 2004 *Mat. Sci. & Eng. A* **375-377** 38
- [7] N. R. Tao, Z. B. Wang, W. P. Tong, M. L. Sui, J. Lu and K. Lu 2002 *Act. Mat.* **50** 4603
- [8] H.W. Zhang, Z.K. Hei, G. Liu, J. Lu, K. Lu 2003 *Act. Mat.* **51** 1871
- [9] H. Chan, H. Ruan, A. Chen, et J. Lu 2010 *Act. Mat.* **58** 5086
- [10] T. Prezeau, T Muller, E. Dransart, Y Giraud 2011 *Traitements et Matériaux* **412** 37
- [11] G. Kermouche, G. Pacquaut, C. Langlade, J.M. Bergheau 2011 *C. R. Mec.* **339** 552
- [12] D.A. Rigney, L.H. Chen, M.G.S. Naylor and A.R. Rosenfield 1984 *Wear* **100** 195
- [13] C. Suryanarayana, E. Ivanov, V.V. Boldyrev 2001 *Mat. Sci. & Eng. A* **304-306** 151
- [14] S. Lamri, C. Langlade, G. Kermouche, V. Martinez 2010 *Mat. Sci. & Eng. A* **527** 7912.
- [15] A. Sekkal, C. Langlade, A.B. Vannes 2002 *Trib. Let.* **15** 265.
- [16] D. Orlov, Y. Todaka, M. Umemoto, T. Nobuhiro 2009 *Mat. Sci. & Eng. A* **499** 427
- [17] C.F. Gu, L.S. Toth, B. Beausir, 2011 *Scr. Mat.* **65** 167
- [18] F. Montheillet, O. Lurdos, G. Damamme 2009 *Act. Mat.* **57** 1602
- [19] L. S. Tóth, Y. Estrin, R. Lapovok, C. Gu 2010 *Act. Mat.* **58** 1782
- [20] C.F. Gu, L.S. Toth, B. Beausir 2012 *Scr. Mat.* **66** 250
- [21] Gourdet S and Montheillet F 2003 *Acta Mater.* **51** pp 2685-2699
- [22] G. Kermouche, F. Grange, C. Langlade 2013 *Mat. Sci. & Eng. A* **569** 71
- [23] G. Kermouche, J.L. Loubet, J.M. Bergheau 2005 *C. R. Mec.* **333** 389
- [24] G. Kermouche, J. L. Loubet, J. M. Bergheau 2008 *Mec. Mat.* **40** 271
- [25] S. P. Jaspers, J. H. Dautzenberg 2002 *J. Mat. Proc. Tech.* **122** 322